The Journal of Physical Chemistry A

 VOLUME 103, NUMBER 31, AUGUST 5, 1999

LETTERS

Semiclassical Tunneling Rates from Ab Initio Molecular Dynamics

M. Ben-Nun and Todd J. Martínez*

Department of Chemistry and the Beckman Institute, University of Illinois, Urbana, Illinois 61801

Received: March 15, 1999; In Final Form: May 24, 1999

We demonstrate a new ab initio semiclassical technique for investigating tunneling effects. Using a semiclassical approach, the method incorporates tunneling effects into first principles molecular dynamics. We apply the method to the intramolecular proton transfer in malonaldehyde and find good agreement with the experimentally measured tunneling splitting. This agreement suggests a wide applicability of the new method to proton transfer and coupled electron−proton transfer processes.

Introduction

In molecules containing both hydrogen donor and acceptor groups in close proximity, an intramolecular hydrogen bond is formed and the hydrogen atom may tunnel between the donor and acceptor groups. Malonaldehyde serves as a textbook example for such intramolecular hydrogen bonding and the theoretical interest in this molecule has been supplemented by a series of spectroscopic studies.[1−7] Most of the theoretical work on malonaldehyde is based on approximate two-dimensional potential energy surfaces,[8−11] although Thompson and co-workers have recently investigated a full-dimensionality model.[12]

Both the height and the width of the barrier through which the proton tunnels often depend very strongly on the motion of all the atoms in the molecule. Consequently, tunneling rates can be extremely sensitive to the potential energy surface that is employed, irrespective of the degree of sophistication of the method that is used to predict the splitting. Thus, when experimental data is available, one expects that tunneling dynamics will provide a sensitive probe of potential energy surfaces near the barrier region.

Proton transfer and coupled electron−proton transfer are important in many biochemical processes, for example, glycolysis and oxidative phosphorylation. There is therefore much interest in simulating such reactions. However, there are two main stumbling blocks in the molecular modeling of proton transfer. The quantum mechanical nature of the nuclei must be confronted to include zero-point and tunneling effects and at the same time the potential energy surfaces must be capable of describing bond rearrangement. The latter is often quite awkward in the context of analytic empirical functions. The empirical valence bond approach of Warshel and Weiss[13] provides a solution to this problem that has recently become particularly popular in studies of the excess proton in water.[14−16] The primary difficulty is that all bond rearrangements which will be allowed must be enumerated explicitly, leading to complications when studying proton transport. The dissociable water potential of Stillinger and co-workers[17−19] avoids this problem and it has also seen recent use.[20,21] However, the increased flexibility comes at the cost of uncertain accuracy. An attractive option is "on-the-fly" solution of the electronic Schrödinger equation, sometimes called "direct dynamics." Truhlar and co-workers have investigated the use of semiempirical methods for this purpose, but found that accurate results usually require explicit re-parametrization for specific reactions.[22] Molecule-specific parametrization or fitting is avoided in ab initio molecular dynamics.[23−25] Several workers have applied ab initio molecular dynamics to hydrogen-bonded systems, but these have been restricted to either classical Newtonian dynamics[26,27] or equilibrium (imaginary time) quantum mechanics.[28,29] Over the past few years, we have pioneered ab initio real-time quantum

* Author to whom correspondence should be addressed.

10.1021/jp990904a CCC: $18.00
Published on Web 07/20/1999

dynamics.[30−36] We have emphasized the case of quantum effects due to electronic nonadiabaticity, but have also shown that these methods can be applied successfully to treat tunneling effects.[37] Recently, the Voth group has also begun to pursue the goal of ab initio real-time quantum dynamics.[38]

In this paper, we concentrate on a slightly less ambitious goal. We do not insist on quantum nuclear dynamics, but instead use a semiclassical formalism to describe the quantum mechanical tunneling events, coupled with "on-the-fly" solution of the electronic Schrödinger equation. The semiclassical method used[9,12,39] bears a resemblance to surface-hopping[40] procedures, with the tunneling event described by trajectories instantaneously hopping under the barrier from one turning point to another. It has been improved somewhat by Keshavamurthy and Miller,[41] but judging from the performance of the original method in two-dimensional model problems,[9] we saw no compelling reason to go beyond the original, simpler method in this work. By solving the electronic Schrödinger equation at each point in time, during the propagation, the required potential energy surfaces are generated "on-the-fly" and the rearrangement of the hydrogen bond is accomplished smoothly (without any input parameters). This ab initio semiclassical technique turns out to be very accurate in the test case used here, where high-quality experimental information is available. Because the semiclassical formalism is much less costly than fully quantum dynamics, there is considerable practical advantage to the method. The work presented here is the first use of ab initio molecular dynamics to evaluate tunneling rates.

Theory

The semiclassical treatment of the tunneling rate used in this work has been presented previously,[12,39] and we give only a brief discussion here. The method is based on the procedure suggested by Makri and Miller,[9] and can be viewed as a classical trajectory/WKB approach. The semiclassical/WKB expression for the tunneling splitting in a one-dimensional double well is given by[42,43]

$$\Delta E = 2\hbar \upsilon e^{-\theta} \tag{1}$$

where υ is the frequency of the oscillator at a total energy E, and θ is the classical action integral through the barrier

$$\theta = \frac{1}{\hbar}\int_{x<}^{x>} \sqrt{2m[V(x) - E]}\,\mathrm{d}x \tag{2}$$

The limits of the integral in eq 2 are the classical turning points (at total energy E) on the two sides of the barrier. As discussed in ref 9, one can express the tunneling splitting (ΔE) in terms of the time derivative of the averaged net tunneling amplitude

$$\Delta E = 2\hbar \frac{\mathrm{d}}{\mathrm{d}t}\langle S_{\mathrm{net}}(\mathrm{t})\rangle \tag{3}$$

where

$$S_{\mathrm{net}}(t) = \sum_n h(t - t_n)e^{-\theta_n} \tag{4}$$

The bracket in eq 3 implies an ensemble average over the initial vibrational phase. The times that a classical trajectory is at a turning point along the tunneling direction x are denoted t_n and $h(\xi)$ is the usual step function: $h(\xi) = 1$ if $\xi > 0$, and $h(\xi) = 0$ if $\xi < 0$.

Equations 1−4 provide the prescription for the semiclassical approach: a classical trajectory is propagated and the magnitude of the momentum of the tunneling particle along the tunneling coordinate, x, is monitored. Each time that a classical turning point is reached, the tunneling integral is computed using eq 2. For each trajectory the net (i.e., cumulative) tunneling amplitude is given by the sum of these instantaneous tunneling amplitudes (eq 4) and the results are averaged over the initial phase. Thus, in the semiclassical picture, tunneling is instantaneous in real time and conserves the momentum of all the particles. This strict sudden approximation poses a problem for symmetric double-well systems for the following reason: when passing from one well to the other the position of all the atoms should be symmetrically reflected. However, within the sudden approximation, the positions of all atoms except the tunneling particle are kept fixed during the tunneling "event." To overcome this difficulty, Thompson and co-workers[12] suggested evaluating only half of the integral, from the inner turning point ($x_<$) to a point x_{sym} where $r_{\mathrm{OH}} = r_{\mathrm{O}\cdots\mathrm{H}}$. The result is then doubled. This leads to a discontinuous derivative in the integrand at x_{sym}, and is thus not wholly satisfactory. However, it does provide a workable solution whose accuracy may be similar to that of the sudden approximation itself. Therefore, we adopt this suggestion in this work.

A complete description of the semiclassical model requires a specification of the tunneling path. The "optimal" choice of this path has been the topic of many papers[44−47] and a variety of choices (e.g., least-action, minimum energy, and straight line paths) have been investigated. In general, one expects the tunneling path to be curved toward the transition state and the choice of a simple straight line (in the full-dimensional coordinate space) is an approximation whose accuracy will vary from molecule to molecule. Nevertheless, since in the present case of malonaldehyde there is no obvious choice for a curved path, we have chosen the tunneling path to be a straight line parallel to the equilibrium O−O distance vector. Other, more sophisticated, choices may be the subject of future investigation.

Time-independent ab initio quantum mechanical studies on malonaldehyde indicate that the Hartree−Fock (HF) approximation is inadequate. The predicted O···H distance (1.88 Å), which is clearly of crucial importance to the tunneling dynamics, is in poor agreement with the value (1.68 Å) deduced from experiment.[5] Adding electron correlation effects via perturbation theory (MP2) yields a structure[48] that is in good agreement with experiment (O···H distance 1.69 Å) and a barrier height for proton transfer of 3.6 kcal/mol. The "best" estimate for the barrier is due to Barone and Adamo[49] who, using the G2 method and B3LYP/DZP geometries, predicted a barrier height of 4.3 kcal/mol. They compared post-HF and DFT methods and concluded that, among the less demanding methods, the best results are obtained by a hybrid DFT/HF approach. In particular, the B3LYP method provides accurate structural parameters and minimizes one of the serious drawbacks of DFT methods—the over-stabilization of structures in which a hydrogen atom is shared between two electronegative atoms. In the following simulations, we use the B3LYP/DFT method with double-ζ basis sets.[50,51] The equilibrium and transition state (TS) structures at this level of theory are shown in Figure 1 as well as the potential along the intrinsic reaction coordinate (IRC), computed with *Gaussian 98*.[52] The predicted theoretical equilibrium geometry is compared with the experimental microwave structure of Wilson et al.[2] (numbers in parentheses). In general the agreement is quite good and in particular the O···H distance is within 0.04 Å of the experimental value. The tendency of DFT methods to overestimate electron correlation leads to an underestimation of the energy barrier for proton transfer. For

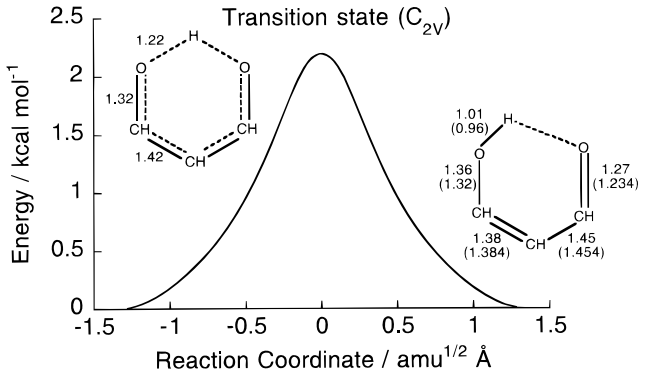

Figure 1. Energy profile (B3LYP) along the intrinsic reaction coordinate for symmetric hydrogen transfer in malonaldehyde. The theoretical equilibrium geometry (right inset) is compared with the experimental structure of Wilson et al.[2] (numbers in parentheses). The predicted transition state structure lies 2.3 kcal/mol above the equilibrium geometry. All bond distances are in Å and the reaction coordinate is expressed as a mass-weighted Cartesian displacement from the transition state structure.

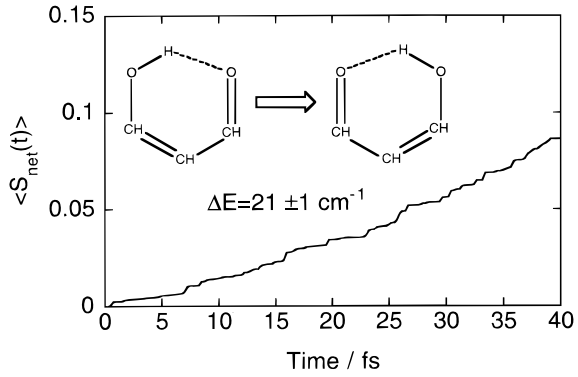

Figure 2. Average net tunneling amplitude as a function of time in femtoseconds. Results are for an ensemble of 150 trajectories and the splitting derived from this curve is 21 ± 1 cm^{-1}, to be compared with the experimental value[2,6,7] of 21.6 cm^{-1}.

example, the BLYP and BP functionals predict energy barriers of 1.0 and 0.4 kcal/mol, respectively.[49] This effect is strongly reduced when including exact exchange (B3LYP), but not completely eliminated judging from the resulting barrier height of 2.3 kcal/mol.

Results and Discussion

The tunneling splitting was calculated using eqs 1−4. A modified version of the Jaguar[53] code was employed to compute the electronic structure and semiclassical dynamics. An ensemble of 150 trajectories was propagated using a velocity Verlet algorithm and a time step of 0.25 fs. At each point in time and for each trajectory, the necessary potential energies and gradients were obtained by solving the electronic Schrödinger equation. The initial conditions were sampled as appropriate for the molecule in the ground vibrational state. Zero-point energy was deposited in each normal mode, and the phases were chosen according to the usual quasi-classical procedure.[54] To ensure that this initial state remains approximately unchanged (i.e., zero-point energy does not flow between modes and classical barrier crossing does not occur) a short run time of 50 fs was used. Within this time duration, approximately four tunneling events were observed for each trajectory.

We have calculated the tunneling splitting (eq 3) from the average net tunneling amplitude shown in Figure 2. The calculated splitting, 21 ± 1 cm^{-1}, is in excellent agreement with

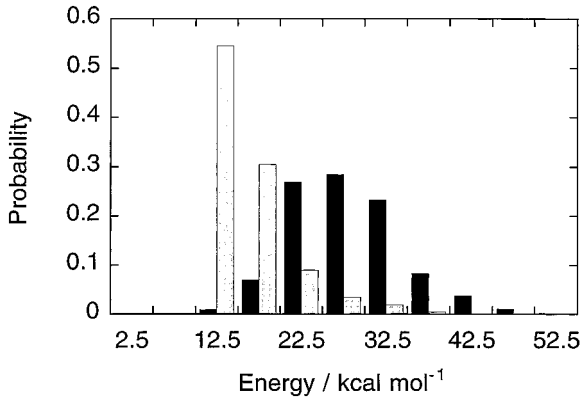

Figure 3. Histogram plots of the distribution of barrier heights (black boxes) and of the product of this distribution with the average tunneling amplitude as a function of energy (gray boxes). (The barrier height is defined as the difference in energy between $x_<$ and x_{sym}.) Both were computed by averaging over all the tunneling events (each trajectory experienced approximately four turning points during the simulation time and we propagated 150 trajectories). As discussed in the text, the second distribution (gray boxes) serves as a measure for the barrier height experienced by trajectories which successfully tunnel.

the experimental value,[2,6,7] 21.6 cm^{-1}. Although traces of the steplike behavior of individual trajectories are present in Figure 2, these would disappear given a larger ensemble. To estimate the accuracy of the calculation, we have (I) computed the splitting using seven randomly chosen sub-ensembles of 80, 100, and 120 trajectories and (II) fitted the data up to 35, 40, and 45 fs. Both procedures result in an error bar of ±1 cm^{-1} and the specific value of the splitting that we report is for the full 150 trajectories and an integration period of 40 fs.

The quantitative agreement between calculation and experiment is somewhat surprising. Although the B3LYP method provides quite accurate structural parameters (when compared to the HF method and/or BLYP and BP functionals), it also underestimates the barrier height for proton transfer (see Figure 1). Moreover, similar agreement (21.8 cm^{-1}) has been reported by Thompson and co-workers[12] using a parametrized PES with a much larger barrier height (10 kcal mol^{-1}) and a very similar width along the IRC. Since this previous work used the same semiclassical treatment of the dynamics, the final agreement of the tunneling splitting may be puzzling. However, the important point to note is that the dominant factor in determining the tunneling splitting is *not* the barrier height along the IRC, but an effective barrier height, i.e., the barrier experienced by the trajectories that have a nonnegligible contribution to the tunneling amplitude. This effective barrier height must be similar in the B3LYP and parametrized PESs. (The effective barrier width is also important. However, the width of the IRC in the two PESs is similar. Hence, the effective widths are likely also very similar.) As a measure for the height of the effective barrier we have computed the distribution of barrier heights and the product of this distribution with the average tunneling amplitude (as a function of barrier height). The second distribution serves as a measure for the effective barrier height (because it weights each barrier height by its average tunneling probability). Since the effective barrier height is a product of two functions: one rapidly decreasing with energy (tunneling amplitude) and one centered at ∼27 kcal/mol (barrier heights), its magnitude (∼12 kcal/mol) is determined (as expected) by the low energy tail of the distribution of barrier heights. Figure 3 suggests that the relevant barrier height is actually 12−15 kcal/mol, much higher than the barrier along the IRC.

Thompson and co-workers have pointed out that the effective

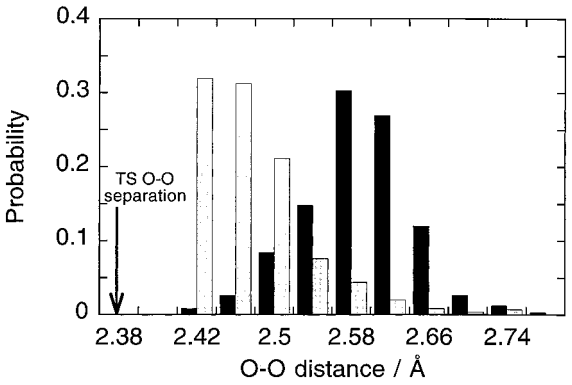

Figure 4. Histogram plots of the distribution of O−O distances when a turning point is reached along the tunneling coordinate (black boxes) and the product of this distribution with the tunneling probability (gray boxes). Distributions are computed as in Figure 3. The arrow denotes the O−O distance of the proton-transfer transition state.

barrier to proton transfer is reduced when r_{oo} is contracted from its equilibrium value, and they thus argue for an effective barrier which is *lower* than that along the IRC. We have verified that this correlation between r_{oo} and the effective barrier is also observed on the B3LYP potential energy surface. However, the dynamical simulations show an effective barrier that is *larger* than the barrier along the IRC. Therefore, we have examined the r_{oo} distances at configurations with high tunneling probabilities. The results are shown in Figure 4, where we plot the probability of reaching a turning point at a given r_{oo} and this probability weighted by the tunneling probability. As expected, tunneling occurs preferentially at the smallest r_{oo}, but these are always *expanded* relative to the transition state (r_{oo} of the TS is denoted with an arrow in Figure 4). Thus, the effective barrier is higher than the barrier along the IRC simply because the molecule does not visit configurations where r_{oo} is similar to that of the transition state. This is a reflection of the rigidity of the heavy atom framework in the molecule, and may be quite common for intramolecular proton transfer.

It is uncertain whether the excellent agreement with experiment obtained here will carry over to proton transfer in other molecules. We may benefit in part from a cancellation of errors—the straight-line tunneling path will tend to increase the effective barrier height for each tunneling event while the B3LYP method underestimates the potential energy in the barrier region. Since it is not yet possible to carry out exact quantum mechanical full-dimensional calculations for molecules of this size, further application of the ab initio semiclassical tunneling model where experimental data is available will be required to determine its expected accuracy.

In summary, we have demonstrated the first dynamical calculation of ab initio semiclassical tunneling rates, and applied it to proton transfer in malonaldehyde. Proceeding entirely from first-principles, we have obtained excellent agreement with the experimentally measured tunneling splitting. This new method provides a promising approach to study proton-transfer problems, which will be the subject of future investigations.

Acknowledgment. We thank Profs. N. Makri and D. L. Thompson for useful discussions. T.J.M. thanks the University of Illinois for start-up funds, the National Science Foundation for a CAREER award, and Research Corporation for a Research Innovation Award. This work was partially supported by NIH (P41 RR05969), NSF (CHE-97-33403), and Research Corporation (RI-0085).

References and Notes

(1) Rowe, W. F.; Duerest, R. W.; Wilson., E. B. *J. Am. Chem. Soc.* **1976**, *98*, 4021.
(2) Baughcum, S. L.; Duerst, R. W.; Rowe, W. F.; Smith, Z.; Wilson, E. B. *J. Am. Chem. Soc.* **1981**, *103*, 6296.
(3) Smith, Z.; Wilson, E. B.; Duerst, R. W. *Spectrochim. Acta, Part A* **1983**, *39*, 1117.
(4) Baughcum, S. L.; Smith, Z.; Wilson, E. B.; Duerst, R. W. *J. Am. Chem. Soc.* **1984**, *106*, 2260.
(5) Turner, P.; Baughcum, S. L.; Coy, S. L.; Smith, Z. *J. Am. Chem. Soc.* **1984**, *106*, 2265.
(6) Firth, D. W.; Beyer, K.; Dvorak, M. A.; Reeve, S. W.; Grushow, A.; Leopold, K. R. *J. Chem. Phys.* **1991**, *94*, 1812.
(7) Baba, T.; Tanaka, T.; Morino, I.; Yamada, K. M. T.; Tanaka, K. *J. Chem. Phys.* **1999**, *110*, 4131.
(8) Carrington, T.; Miller, W. H. *J. Chem. Phys.* **1986**, *84*, 4364.
(9) Makri, N.; Miller, W. H. *J. Chem. Phys.* **1989**, *91*, 4026.
(10) Bosch, E.; Moreno, M.; Lluch, J. M.; Bertran, J. *J. Chem. Phys.* **1990**, *93*, 5685.
(11) Benderskii, V. A.; Makarov, D. E.; Grinevich, P. G. *Chem. Phys.* **1993**, *170*, 275.
(12) Sewell, T. D.; Guo, Y.; Thompson, D. L. *J. Chem. Phys.* **1995**, *103*, 8557.
(13) Warshel, A.; Weiss, R. M. *J. Am. Chem. Soc.* **1980**, *102*, 6218.
(14) Lobaugh, J.; Voth, G. A. *J. Chem. Phys.* **1996**, *104*, 2056.
(15) Sagnella, D. E.; Tuckerman, M. E. *J. Chem. Phys.* **1998**, *108*, 2073.
(16) Vuilleumier, R.; Borgis, D. *J. Phys. Chem.* **1998**, *102*, 4261.
(17) Stillinger, F. H.; David, C. W. *J. Chem. Phys.* **1978**, *69*, 1473.
(18) Stillinger, F. H. *J. Chem. Phys.* **1979**, *71*, 1647.
(19) Weber, T. A.; Stillinger, F. H. *J. Phys. Chem.* **1982**, *86*, 1314.
(20) Pomes, R.; Roux, B. *J. Phys. Chem.* **1996**, *100*, 2519.
(21) Drukker, K.; de Leeuw, S. W.; Hammes-Schiffer, S. *J. Chem. Phys.* **1998**, *108*, 6799.
(22) Liu, Y.-P.; Lu, D.; Gonzalez-Lafont, A.; Truhlar, D. G.; Garret, B. C. *J. Am. Chem. Soc.* **1993**, *115*, 5.
(23) Car, R.; Parrinello, M. *Phys. Rev. Lett.* **1985**, *55*, 2471.
(24) Hartke, B.; Carter, E. A. *Chem. Phys. Lett.* **1992**, *189*, 358.
(25) Parrinello, M. *Solid State Commun.* **1997**, *102*, 107.
(26) Tuckerman, M.; Laassonen, K.; Sprik, M.; Parrinello, M. *J. Chem. Phys.* **1995**, *103*, 150.
(27) Cheng, H.-P.; Krause, J. L. *J. Chem. Phys.* **1997**, *107*, 8461.
(28) Tuckerman, M. E.; Marx, D.; Klein, M. L.; Parrinello, M. *Science* **1997**, *275*, 817.
(29) Miura, S.; Tuckerman, M. E.; Klein, M. L. *J. Chem. Phys.* **1998**, *109*, 5290.
(30) Martínez, T. J.; Levine, R. D. *Chem. Phys. Lett.* **1996**, *259*, 252.
(31) Martínez, T. J.; Levine, R. D. *J. Chem. Phys.* **1996**, *105*, 6334.
(32) Martínez, T. J. *Chem. Phys. Lett.* **1997**, *272*, 139.
(33) Martínez, T. J.; Ben-Nun, M.; Levine, R. D. *J. Phys. Chem.* **1997**, *101*, 1A, 6389.
(34) Ben-Nun, M.; Martínez, T. J. *J. Chem. Phys.* **1998**, *108*, 7244.
(35) Ben-Nun, M.; Martínez, T. J. *Chem. Phys. Lett.* **1998**, *298*, 57.
(36) Ben-Nun, M.; Martínez, T. J. *J. Chem. Phys.* **1999**, *110*, 4134.
(37) Ben-Nun, M.; Martínez, T. J. In preparation.
(38) Pavese, M.; Berard, D. R.; Voth, G. A. *Chem. Phys. Lett.* **1999**, *300*, 93.
(39) Guo, Y.; Thompson, D. L. *J. Chem. Phys.* **1996**, *105*, 7480.
(40) Tully, J. C. *J. Chem. Phys.* **1990**, *93*, 1061.
(41) Keshavamurthy, S.; Miller, W. H. *Chem. Phys. Lett.* **1993**, *205*, 96.
(42) Ford, K. W.; Hill, D. L.; Wakano, M.; Wheeler, J. A. *Ann. Phys.* **1959**, *7*, 239.
(43) Miller, W. H. *J. Chem. Phys.* **1979**, *83*, 960.
(44) Marcus, R. A.; Coltrin, M. E. *J. Chem. Phys.* **1977**, *67*, 2609.
(45) Cerjan, C. J.; Shi, S.; Miller, W. H. *J. Phys. Chem.* **1982**, *86*, 2244.
(46) Truhlar, D. G.; Isaacson, A. I.; Garrett, B. C. Generalized Transition State Theory. In *Theory of Chemical Reaction Dynamics*; Baer, M., Ed.; CRC Press: Boca Raton, FL, 1985; Vol. 4.
(47) Lynch, G. C.; Truhlar, D. G.; Garrett, B. C. *J. Chem. Phys.* **1989**, *90*, 3102.
(48) Frisch, M. J.; Scheiner, A. C.; Shaefer, H. F., III; Binkley, J. S. *J. Chem. Phys.* **1985**, *82*, 4194.
(49) Barone, V.; Adamo, C. *J. Chem. Phys.* **1996**, *105*, 11007.
(50) Dunning, T. H., Jr.; Hay, P. J. Gaussian Basis Sets for Molecular Calculations. In *Modern Theoretical Chemistry: Methods of Modern Electronic Structure Theory*; Schaefer, H. F., III, Ed.; Plenum: New York, 1977; Vol. 3, p 1.
(51) *Gaussian Basis Sets for Molecular Calculations*; Huzinaga, S., Ed.; Elsevier: Amsterdam, 1984.
(52) Frisch, M. J.; Trucks, G. W.; Schlegel, H. B.; Scuseria, G. E.; Robb, M. A.; Cheesman, J. R.; Zakrzewski, V. G.; Montgomery Jr., J. A.; Stratmann, R. E.; Burant, J. C.; Dapprich, S.; Millam, J. M.; Daniels, A.

D.; Kudin, K. N.; Strain, M. C.; Farkas, O.; Tomasi, J.; Barone, B.; Cossi, M.; Cammi, R.; Mennucci, B.; Pomelli, C.; Adamo, C.; Clifford, S.; Ochterski, J.; Petersson, G. A.; Ayala, P. Y.; Cui, Q.; Morokuma, K.; Malick, D. K.; Rabuck, A. D.; Raghavachari, K.; Foresman, J. B.; Cioslowski, J.; Oritiz, J. V.; Stefanov, B. B.; Liu, G.; Liashenko, A.; Piskorz, P.; Komaromi, I.; Gomperts, R.; Martin, R. L.; Fox, D. J.; Keith, T.; Al-Laham, M. A.; Peng, C. Y.; Nanayakkara, A.; Gonzalez, C.; Challacombe, M.; Gill, P. M. W.; Johnson, B.; Chen, W.; Wong, M. W.; Andres, J. L.; Gonzalez, C.; Head-Gordon, M.; Replogle, E. S.; Pople, J. A. *Gaussian 98*, Revision A.1; *Gaussian 98*, Revision A.1 ed.; Gaussian, Inc.: Pittsburgh, 1998.

(53) *Jaguar v3.5*; Schrodinger, Inc.: Portland, OR, 1998.

(54) Truhlar, D. G.; Muckerman, J. T. Reactive scattering cross sections III: quasiclassical and semiclassical methods. In *Atom-Molecule Collision Theory*; Bernstein, R. B., Ed.; Plenum: New York, 1979; p 505.